

## RESEARCH ARTICLE

# P63 targeted deletion under the FOXP1 promoter disrupts pre- and post-natal thymus development, function and maintenance as well as induces severe hair loss

Heather E. Stefanski<sup>1</sup>, Yan Xing<sup>1</sup>, Jemma Nicholls<sup>1</sup>, Leslie Jonart<sup>1</sup>, Emily Goren<sup>1</sup>, Patricia A. Taylor<sup>1</sup>, Alea A. Mills<sup>2</sup>, Megan Riddle<sup>1</sup>, John McGrath<sup>3</sup>, Jakub Tolar<sup>1</sup>, Georg A. Hollander<sup>4,5,6</sup>, Bruce R. Blazar<sup>1\*</sup>

**1** Division of Blood and Marrow Transplantation, Department of Pediatrics, University of Minnesota, Minneapolis, MN, United States of America, **2** Cold Spring Harbor Laboratory, Cold Spring Harbor, New York, New York, United States of America, **3** Molecular Dermatology, St John's Institute of Dermatology, King's College, London, England, **4** Department of Paediatrics, University of Oxford, Oxford, United Kingdom, **5** Department of Biomedicine, Basel University Children's Hospital, University of Basel, Basel, Switzerland, **6** Department of Biosystems Science and Engineering, ETH Zurich, Basel, Switzerland

\* [blaza001@umn.edu](mailto:blaza001@umn.edu)



## OPEN ACCESS

**Citation:** Stefanski HE, Xing Y, Nicholls J, Jonart L, Goren E, Taylor PA, et al. (2022) P63 targeted deletion under the FOXP1 promoter disrupts pre- and post-natal thymus development, function and maintenance as well as induces severe hair loss. PLoS ONE 17(1): e0261770. <https://doi.org/10.1371/journal.pone.0261770>

**Editor:** Subhasis Barik, Chittaranjan National Cancer Institute, INDIA

**Received:** June 16, 2021

**Accepted:** December 9, 2021

**Published:** January 25, 2022

**Copyright:** © 2022 Stefanski et al. This is an open access article distributed under the terms of the [Creative Commons Attribution License](https://creativecommons.org/licenses/by/4.0/), which permits unrestricted use, distribution, and reproduction in any medium, provided the original author and source are credited.

**Data Availability Statement:** All relevant data are within the paper and its [Supporting Information](#) files.

**Funding:** This work was supported by National Institutes of Health P01 CA065493; R01 AI081918; R37 AI34495; R01 HL11879 to BRB and Wellcome Trust, 066521 to GH. The funders had no role in study design, data collection and analysis, decision to publish, or preparation of the manuscript.

## Abstract

Progressive immune deficiency of aging is characterized by severe thymic atrophy, contracted T cell repertoire, and poor immune function. p63 is critical for the proliferative potential of embryonic and adult stem cells, as well as thymic epithelial cells (TECs). Because p63 null mice experience rapid post-natal lethality due to epidermal and limb morphogenesis defects, studies to define a role for p63 expression in TEC biology focused on embryonic thymus development and *in vitro* experiments. Since post-natal thymic stromal development and function differs from that of the embryo, we assessed the impact of lineage-restricted p63 loss on pre- and post-natal murine TEC function by generating mice with a loss of p63 function targeted to TEC, termed p63<sup>TECKO</sup> mice. In adult p63<sup>TECKO</sup> mice, severe thymic hypoplasia was observed with a lack in a discernable segregation into medullary and cortical compartments and peripheral T cell lymphopenia. This profound thymic defect was seen in both neonatal as well as embryonic p63<sup>TECKO</sup> mice. In addition to TECs, p63 also plays an important role in the development of stratified epithelium of the skin; lack of p63 results in defects in skin epidermal stratification and differentiation. Interestingly, all adult p63<sup>TECKO</sup> mice lacked hair follicles despite having normal p63 expression in the skin. Together our results show a critical role of TEC p63 in thymic development and maintenance and show that p63 expression is critical for hair follicle formation.

## Introduction

The thymus is essential for the growth, differentiation and selection of T cells whereby thymic epithelial cells (TECs), fibroblasts, B cells and hematopoietic cells constitute its major stromal

**Competing interests:** The authors have declared that no competing interests exist.

cell types enabling normal thymopoiesis to occur [1]. Distinct stages in the intrathymic development of T cells, a.k.a. thymocytes, are distinguished by different cell surface markers including the differential expression of CD4 and CD8. The most immature thymocytes are characterized by a CD4<sup>-</sup>CD8<sup>-</sup> (double-negative, DN) phenotype and yet lack the expression of a complete T cell antigen receptor (TCR). DN thymocytes are resident in the thymic cortex where they differentiate into more mature CD4<sup>+</sup>CD8<sup>+</sup> (double-positive, DP) thymocytes that eventually express a TCR [2] and thus undergo in sequential fashion first positive selection and then a first wave of negative thymocyte selection [3–5]. Thymocytes that have successfully passed these two selection steps access the thymus medulla where a second wave of negative selection either eliminates cells with a high TCR specificity or deviates their development to adopt a T regulatory cell fate. Post-selection, mature thymocytes have either a CD4<sup>+</sup>CD8<sup>-</sup> or CD4<sup>-</sup>CD8<sup>+</sup> single positive (SP) phenotype and after additional maturation are exported from the medulla to the periphery [2].

The p63 transcription factor is a member of the p53 gene family [6] and exerts pleiotropic functions, including cell proliferation, survival, apoptosis, differentiation, senescence, and aging [7,8]. The p63 locus architecture has two promoters, and its transcripts are characteristically subject to alternative splicing generating transactivating (TA-p63) or dominant negative ( $\Delta$ N-p63) isoforms [9].  $\Delta$ N-p63 isoforms are most abundant in mature proliferating epithelia and dramatically downregulated upon differentiation and growth arrest [10].  $\Delta$ N-p63 is expressed in both cortical (c) TEC and medullary (m) TEC [11]. p63 is also critically important for skin development and maintenance and is predominantly found in the bulge of the hair follicle and to a lesser extent in the interfollicular epidermis and hair bulb [12,13].

A role for p63 in TEC biology has been suggested in mice rendered p63 deficient as these animals demonstrated at birth a severely reduced thymus size likely secondary to functional deficiencies of its non-hematopoietic stromal compartment; a supposition that correlates with an increased rate of TECs apoptosis in newborn mice [12,14]. Because mice germ-line deficient in p63 expression die early after birth, quantitative and qualitative studies concerning a role of p63 expression in TEC function and maintenance beyond the neonatal period were not possible [12]. To circumvent this limitation, we generated mice with a TEC-targeted loss of p63 expression to answer the question whether p63 expression is essential for postnatal TEC biology. We report here on the effects of p63 deletion in both the thymus and skin.

## Materials and methods

### Mice

Mice were kept under specific pathogen-free conditions and used according to federal and institutional regulations. To generate p63-deficient TECs, mice with a conditional p63 allele [15] (p63 fl/fl) were crossed to transgenic mice expressing the Cre recombinase under the FoxN1 promoter that drives expression in TECs and skin epithelial cells [16] (both of which are on the C57BL/6 (B6) background, and provided by a co-author, AAM). In mice that are heterozygous for Cre, p63 is deleted in TECs; the p63<sup>+/+</sup> that are Cre<sup>-</sup> express p63 in TECs. Mice that were Cre<sup>+</sup> were considered p63<sup>TECko</sup>; mice that were Cre<sup>-</sup> were considered p63<sup>+/+</sup> and are denoted as such. To determine which mice had TEC p63 deficiency in the embryonic experiments, p63<sup>TECko</sup> mice were genotyped using DNA from tail clippings on embryonic day 15.5 (E15.5) (day 1 is day of gestation), as previously described [15]. All murine studies were conducted under a protocol approved by the University of Minnesota IACUC (protocol 2104-39043A). As outlined in the IACUC protocol, mice were handled humanely and euthanized using the aforementioned University of Minnesota IACUC approved cervical dislocation method to minimize suffering.

## Flow cytometry and cell suspension

Mouse thymus, spleen, and lymph node (LN) were processed into single cell suspensions and analyzed by flow cytometry. Dead cells were stained by a fixable viability dye conjugated to eFluor780 (eBioscience). The following antibodies were purchased from BD biosciences: The following antibodies were purchased from eBioscience: CD3 (145-2C11), CD4 (GK1.5), CD11c (N418), and CD25 (PC61.5). The following antibodies were purchased from BioLegend: CD8 (53-6.7), CD11b (M1/70), CD44 (IM7), CD45 (30-F11), CD62L (MEL-14), NK-1.1 (PK136), Ly-51 (6C3), and UEA-1 were purchased from Vector Laboratories. Anti-activated Caspase-3 antibody (C92-605) was purchased from BD Biosciences. Flow cytometric analysis and cell sorting were performed (FACS Aria) using FACSFortessa (BD Biosciences) and FlowJo software (Tree Star).

## BrdU staining

Mice were injected twice intraperitoneally with 1mg (100  $\mu$ l/mouse) Bromodeoxyuridine (BrdU, BD Bioscience) within 4 hours. One day later, BrdU incorporation was analysed by flow cytometry using the BrdU Flow Kit according to manufacturer's protocol (BD Bioscience).

## Immunohistochemistry

Intact thymi embedded in optimum cutting temperature (OCT) compound (Sakura, Tokyo, Japan) were snap-frozen in liquid nitrogen and stored at  $-80^{\circ}\text{C}$ . Cryosections (7  $\mu$ m) were fixed by air-drying overnight, blocking with 10% normal horse serum/PBS (Jackson ImmunoResearch Laboratories, West Grove, PA), and staining with rabbit-anti-mouse cytokeratin-5 (K5) antibody (Covance, Berkeley, CA) plus a cychrome-5-conjugated goat-anti-rabbit antibody (Invitrogen) and biotinylated mouse-anti-mouse K18 (Progen Biotechnik, Heidelberg, Germany) plus Alexa Fluor 555-conjugated streptavidin (Invitrogen), p63 (4A4, Santa Cruz Biotechnology). Sections were mounted under a cover slip with 4,6-diamidino-2-phenylindole anti-fade solution (Invitrogen) and imaged on the following day at room temperature using an Olympus FluoView 500 Confocal Scanning Laser Microscope (Olympus, Center Valley, PA). Immunofluorescence for Cre+ and Cre- mice.

Immunofluorescent staining was performed on unaffected and affected skin and thymus samples. Affected skin was identified as having no hair or patchy hair. Unfixed tissue was prepared for sectioning by freezing in optimal cutting temperature (OCT, Sakura Finetek USA, Torrance, CA). Tissue sections were cut at 6  $\mu$ m on a cryostat and placed on positively charged glass slides. Sections were fixed in room temperature acetone for 5 minutes, rehydrated in 1x PBS, permeabilized with 0.2% Triton X for 10 minutes followed by blocking with 10% normal donkey serum for 1 hour (Jackson ImmunoResearch, West Grove, PA). Primary antibodies p63 (Boster Biological, Pleasanton, CA, 1:200), Keratin 5 and Loricrin (Biolegend, San Diego, CA, 1:500, 1:200), Ki67 (Abcam, Burlingame, CA, 1:200), CK18 (LifeSpan Biosciences, Seattle, WA 1:200), and Epcam1 Fitc (eBioscience, San Diego, CA 1:100) were applied for 1.5 hours. Corresponding secondary antibodies donkey anti-rabbit cy3 (Jackson ImmunoResearch, West Grove, PA 1:500), and Alexa Fluor 488 goat anti-chicken, Alexa Fluor 488 goat anti-rat (Molecular Probes, Eugene, OR, 1:800) were used. All incubations were done at room temperature. Slides were cover slipped with hard set DAPI, 4,6-diamidino-2-phenylindole, (Vector Labs, Burlingame, CA) and examined by confocal fluorescence microscopy (Olympus BX61, Olympus Optical, Tokyo, Japan).

## TEC isolation

TEC single-cell suspension were prepared and sorted based on CD45<sup>-</sup>EpCAM<sup>+</sup> of cTECs (UEA<sup>-</sup>1-Ly51) and mTECs(UEA-1<sup>+</sup>Ly51<sup>+</sup>I-A<sup>b+</sup>) as previously described [17]. Dead cells were excluded upon a fixable eFluor 780 viability dye staining. UEA-1 and CD45 (30-F11) were

purchased from Vector Laboratories and BD Biosciences, respectively. The following Abs were purchased from eBioscience: CD16/32 (93) and MHC class II (AF6-120.1). The following Abs were purchased from BioLegend: CD326 (Ep-Cam, G8.8) and Ly-51 (6C3). FACS data were collected using BD LSR flow cytometer and were analyzed using FlowJo version 10 (Tree Star).

### Statistical analysis

Statistical analysis was performed using Student *t* test (unpaired, two-tailed). Probability values were classified into four categories:  $p > 0.05$  (NS),  $*0.05 \geq p > 0.01$ ,  $**0.01 \geq p > 0.001$ ,  $***p \leq 0.0001$ , and  $****0.0001 \leq p \leq 0.001$ .

## Results

### Conditional p63 deletion results in catastrophic thymic hypoplasia

To establish a specific role for p63 in TEC development and function, we generated and analyzed mice with a conditional loss of *p63* targeted to all TEC (designated  $p63^{\text{TECKo}}$ ) due to a deletion of *p63* exons 5, 6 and 7 which alters the reading frame and thus affects the function of any protein should it be generated [15]. In embryos at day 15.5 of development (E15.5)  $p63^{\text{TECKo}}$ , p63 was undetectable in TECs using immunohistochemistry and confocal microscopy (Fig 1A), validating our experimental model.

We first sought to assess the effect of p63 deletion on TEC cellularity and architectural organization in 2–4-month-old mice. The thymus  $p63^{\text{TECKo}}$  was significantly smaller in size (Fig 1B) and displayed an abnormal histological architecture in H&E stains with no discernible demarcation between the cortex and medulla (Fig 1C). TECs can be classified based on their positional, structural, antigenic, and functional characteristics either as cTECs (flow cytometrically identified as  $\text{Ly51}^+\text{UEA1}^-$ ) or as mTECs ( $\text{Ly51}^-\text{UEA1}^+$ ) [18]. The architectural organization and composition of the TEC scaffold in cortex and medulla was assessed by immunohistology using anti-keratin antibodies directed at keratin (K)18 for cTECs and K5 for mTECs as well as reactivity to *Ulex europaeus* agglutinin 1 (UEA-1), a lectin that binds to mTECs [18]. A detailed investigation of the epithelial compartment showed that  $p63^{\text{TECKo}}$  had a disorganized structure that lacked individual and well demarcated medullary islands (Fig 1D) a finding that correlated with a loss of a distinct cortico-medullary junction. Fewer TECs were detected in mutant when compared to  $p63^{+/+}$  (Fig 1E;  $p = 0.0022$ ). This reduction affected both the cTEC ( $p = 0.0022$ ) and mTEC population ( $p = 0.0022$ ) (Figs 1F, 1G and S1) and correlates with reduced proliferative potential of TECs in  $p63^{\text{TECKo}}$  mice (S2 Fig). The ratio of cortical to medullary TEC was changed in  $p63^{\text{TECKo}}$  mice secondary to a higher frequency of cTEC ( $p = 0.0022$ ) relative to mTEC ( $p = 0.0022$ ) when compared to  $p63^{+/+}$  mice.

Total thymocyte numbers were also significantly decreased ( $p = 0.0022$ ) and this was seen in all subsets in  $p63^{\text{TECKo}}$  mice (Fig 1H–1J). The decrease in cell number also translated to significant decreases in frequencies of DP ( $p = 0.0077$ ), and CD4 SP ( $p = 0.0297$ ) but not the CD8 SP ( $p = 0.9731$ ) or DN ( $p = 0.9527$ ) subsets in the  $p63^{\text{TECKo}}$  mice (Fig 1I and 1J), as well as significant decreases in the frequency of  $\text{FoxP3}^+$  Treg (S3 Fig;  $p < 0.0001$ ). Taken together, our data shows that p63 expression in TECs is required for the establishment of a normal thymic microenvironment, function and sustained integrity of the thymus.

### P63 deletion in embryonic mice results in decreased TECs and immature thymocytes

Due to the profound defect in adult mice, we wanted to see if we could pinpoint when the thymic defect occurred. In order to accomplish this, E15.5 thymic lobes were examined. As shown

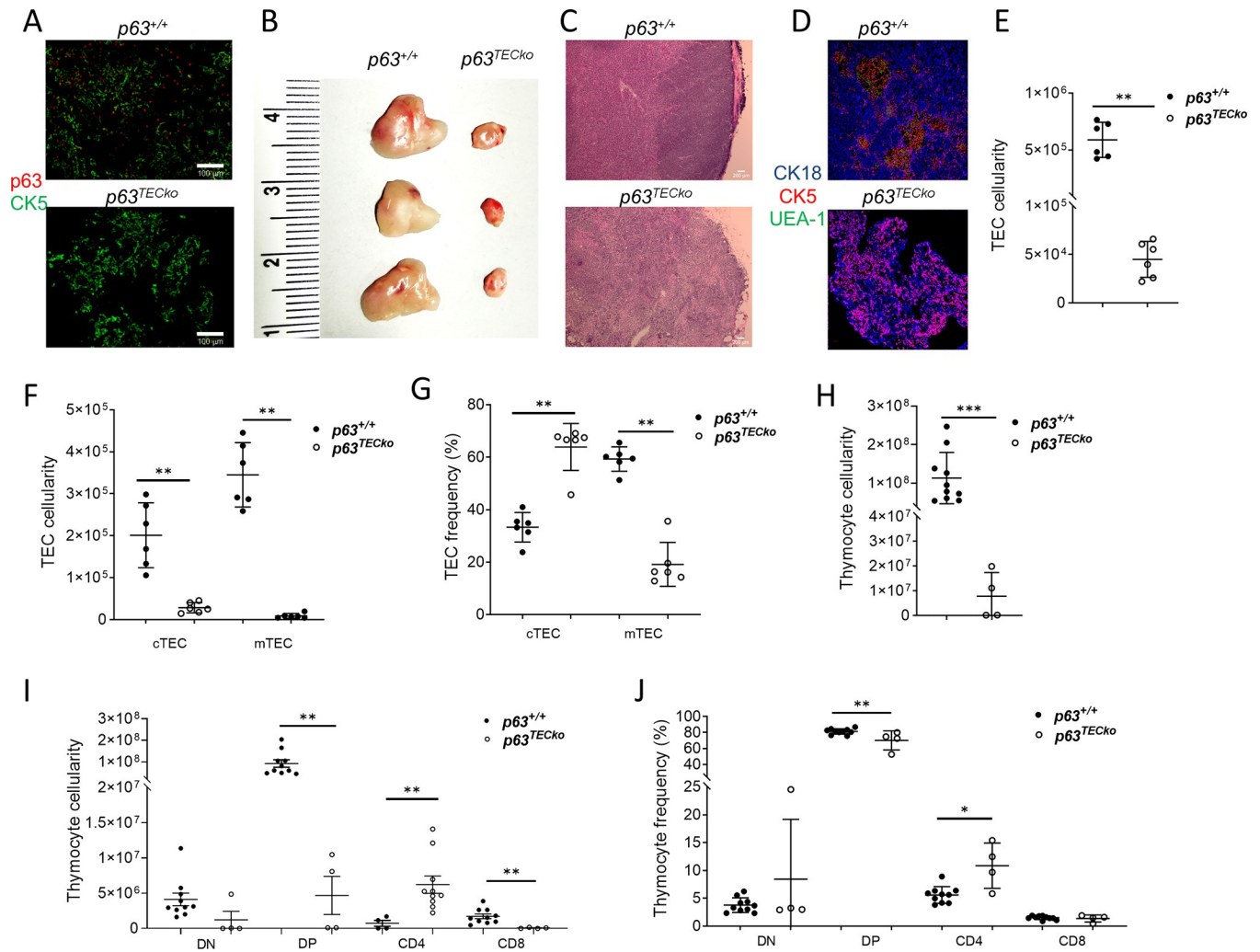


**Fig 1.  $p63^{TECKo}$  mice have profound thymic hypoplasia.** Fig 1A shows absence of p63 in  $p63^{TECKo}$  TECs. Fig 1B shows the thymus size of both  $p63^{+/+}$  and  $p63^{TECKo}$  adult mice. Fig 1C shows H and E staining. The scale bars are 50  $\mu$ m. Fig 1D shows CK18 (blue), CK5 (red) and UEA-1 (green) staining. Absolute numbers of TEC (1E and  $p = 0.0022$ ), of TEC subsets (1F; cTEC,  $p = 0.0022$ ; mTEC,  $p = 0.0022$ ) and frequency of TEC subsets (1G; cTEC,  $p = 0.0022$ ; mTEC,  $p = 0.0022$ ) based on  $(CD45^{-}EpCAM^{+}$  of cTECs ( $Ly51^{+}UEA-1^{-}$ ) and mTECs ( $Ly51^{+}UEA-1^{+}I-A^{b+}$ ) are shown. Flow cytometric analysis for the cell-surface expression of CD4 and CD8 on thymocytes isolated from  $p63^{TECKo}$  and littermate control mice. Numbers denote absolute number of cells of total thymocytes (1H;  $p = 0.0022$ ) and subsets (1I; DP,  $p = 0.0011$ ; CD4,  $p = 0.0077$ ; CD8,  $p = 0.0022$ ), and frequency of the subtypes (1J; DP,  $p = 0.0077$ ; CD4,  $p = 0.0297$ ). P values are shown.

<https://doi.org/10.1371/journal.pone.0261770.g001>

in Fig 2, immunohistochemistry showed that the frequencies of mTECs ( $K5^{+}$ ) but not cTECs ( $K18^{+}$ ) were decreased in  $p63^{TECKo}$  thymus compared to  $p63^{+/+}$  tissue sections (Fig 2A). At E15.5, separate medullary islands had formed in littermate embryos whereas the morphology of the thymic medulla in  $p63^{TECKo}$  mice appeared to be largely positioned in the center of the lobe as a single large aggregate mTEC (Fig 2A). The absolute number of TECs ( $p < 0.0001$ ) was significantly decreased in  $p63^{TECKo}$  mice when compared to  $p63^{+/+}$  (Fig 2B). This reduction affected both the cTEC ( $p = 0.014$ ) and the mTEC ( $p < 0.0001$ ) compartments (Fig 2C). Additionally, the frequencies of cTECs were elevated in the  $p63^{TECKo}$  mice ( $P = 0.0001$ ) whereas the frequencies of mTECs were lower in the  $p63^{TECKo}$  mice ( $p = 0.0008$ ) compared to  $p63^{+/+}$  (Fig 2D). To examine the functional consequences of loss of p63 expression in TECs, we examined thymopoiesis of E15.5  $p63^{TECKo}$  mice using single cell suspensions and analyzed the thymus for CD44 and CD25. As shown in Fig 2E, total thymic cellularity was also decreased in  $p63^{TECKo}$  mice. Immature

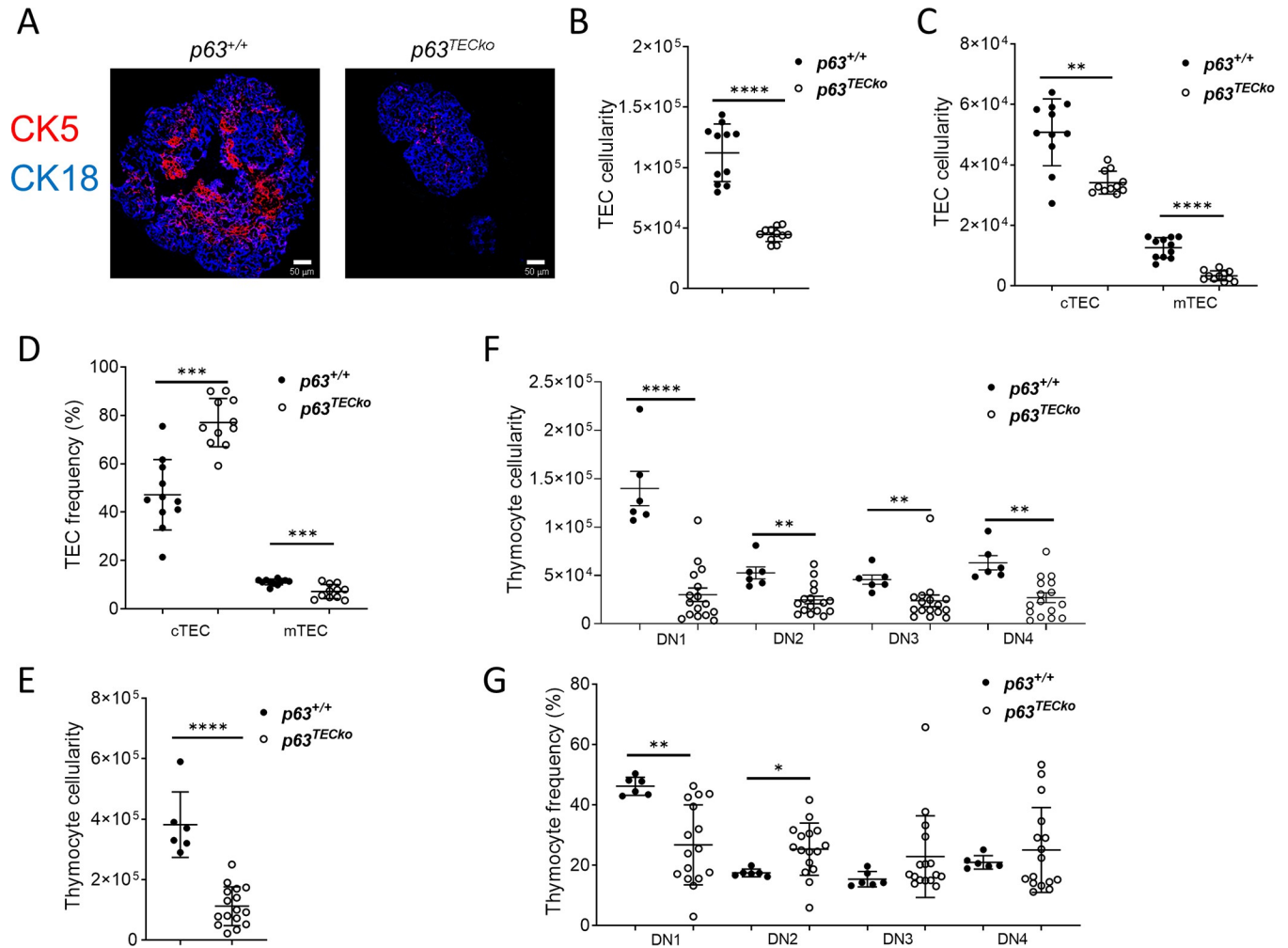


**Fig 2.  $p63^{TECKo}$  mice have decreased TECs and DN1 cells in embryonic mice.** Fig 2A shows CK18 (blue), CK5 (red) staining. The scale bars are 50  $\mu$ m. Absolute TEC cellularity (2B,  $p < 0.0001$ ) numbers of TEC subsets (2C; cTEC,  $p = .0014$ ; mTEC,  $p < 0.0001$ ) and frequency of TEC subsets (2D; cTEC,  $p = 0.001$ ; mTEC,  $p = 0.008$ ) based on (CD45<sup>+</sup>EpCAM<sup>+</sup> of cTECs (Ly51<sup>+</sup>UEA-1<sup>-</sup>) and mTECs (Ly51<sup>+</sup>UEA-1<sup>+</sup>I-A<sup>b+</sup>)) are shown. Flow cytometric analysis for the cell-surface expression of CD44 and CD25 on thymocytes isolated from  $p63^{TECKo}$  and  $p63^{+/+}$  mice. Thymocyte cellularity of total thymocytes (2E,  $p = < 0.0001$ ) and DN subsets (2F; DN1,  $p = 0.0004$ ; DN2,  $p = 0.0151$ ; DN3,  $p = 0.0243$ ; DN4,  $p = 0.0036$ ) frequency of DN subsets (2G; DN1,  $p < 0.0001$ ). This experiment was performed 2 times with at least 3 mice per group. P values are shown.

<https://doi.org/10.1371/journal.pone.0261770.g002>

thymocyte population examined were double negative (DN) cells that are characterized by CD44 and CD25 expression: DN1 (CD25<sup>-</sup>CD44<sup>+</sup>), DN2 (CD25<sup>+</sup>CD44<sup>+</sup>), DN3 (CD25<sup>+</sup>CD44<sup>-</sup>) and DN4 cells (or pre-DP cells; CD25<sup>-</sup>CD44<sup>-</sup>). In assessing the different stages of DN cells, there was a significant decrease in the cellularity of all DN stages (Fig 2F) in  $p63^{TECKo}$ . This decrease in cell number also correlated with a decrease in DN1 frequency in the  $p63^{TECKo}$  mice ( $p < 0.0001$ ; Fig 2G). Taken together, this data shows that decreased TEC numbers and altered thymus architecture affect mainly the most immature DN1 stage of thymocyte development but not yet the more mature DN subsets in embryonic  $p63^{TECKo}$  mice.

### P63 deletion in postnatal TEC compromises thymus function

We next investigated the structural and functional consequences of a lack of p63 expression in TECs in postnatal mice. The thymus architecture in the  $p63^{TECKo}$  mice was very altered based

on CK5 and CK18 staining (Fig 3A); the  $p63^{TECKo}$  mice had minimal staining of both the cortex and medulla due to its small size. In  $p63^{TECKo}$  newborn mice, total TECs ( $p = 0.0079$ ), as well as both cTECs ( $p = 0.0079$ ) and mTECs ( $p = 0.0079$ ), (Fig 3B and 3C respectively) were significantly decreased. Similar to E15.5  $p63^{TECKo}$  mice, the frequency of cTEC was higher ( $p = 0.0079$ ) and mTEC ( $p = 0.0317$ ) was lower in  $p63^{TECKo}$  mice (Fig 3D). The loss of TECs in  $p63^{TECKo}$  had major deleterious effects on thymocyte development. Total thymus cellularity was significantly decreased in  $p63^{TECKo}$  newborn mice as compared to  $p63^{+/+}$  (Fig 3E). This reduction correlated with a marked decrease of all major thymocyte subpopulations (Fig 3F). The frequency of DP cells was significantly lower in  $p63^{TECKo}$  newborn mice ( $p = 0.0328$ ); however, the predominant population is DP cells in the  $p63^{+/+}$  as well as the  $p63^{TECKo}$  newborn mice (Fig 3G). Collectively, this data shows that by the newborn stage, p63 deficiency in TECs has a profound defect in not only thymic architecture, but also thymocyte development.

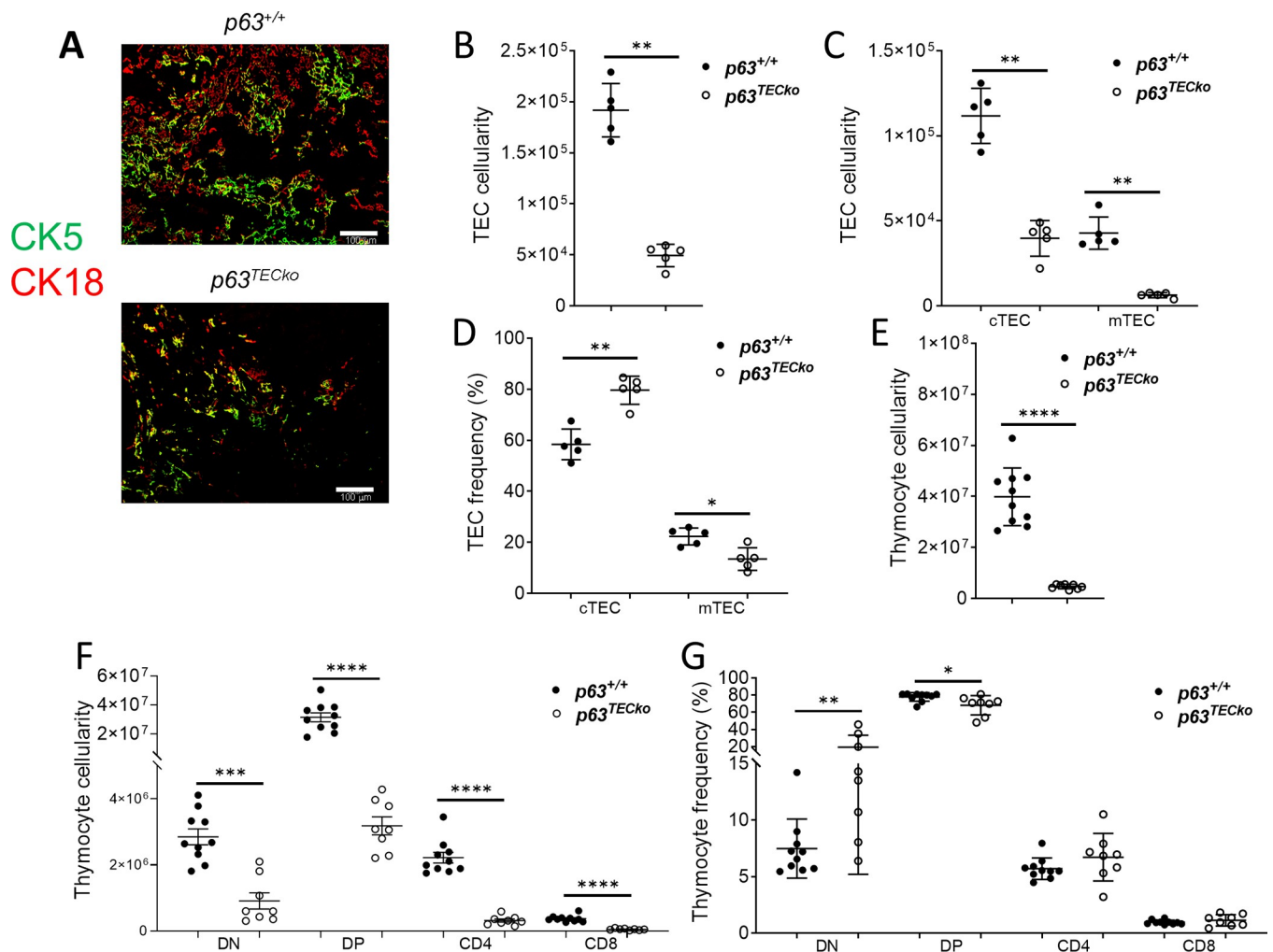


**Fig 3. Newborn  $p63^{TECKo}$  mice have severe thymic hypoplasia.** Fig 3A shows abnormal staining of the thymus in  $p63^{TECKo}$  mice in the CK5 (green) and CK18 (red) compartments. The scale bars are 100  $\mu$ m. Absolute TEC (3B,  $p = 0.0079$ ), numbers of TEC subsets (3C; cTEC,  $p = 0.0079$ ; mTEC,  $p = 0.0079$ ) and frequency of TEC subsets (3D; cTEC,  $p = 0.0079$ ; mTEC,  $p = 0.0317$ ) based on (CD45<sup>+</sup>EpCAM<sup>+</sup> of cTECs (Ly51<sup>+</sup>UEA-1) and mTECs(Ly51<sup>+</sup>UEA-1<sup>+</sup>I-A<sup>b+</sup>) are shown. Flow cytometric analysis for the cell-surface expression of CD4 and CD8 on thymocytes isolated from  $p63^{TECKo}$  and  $p63^{+/+}$  mice. Numbers denote absolute number of total thymocytes (3E,  $p < 0.0001$ ) and subsets (3F; DN,  $p = 0.0002$ ; DP,  $p < 0.0001$ ; CD4,  $p < 0.0001$ ; CD8,  $p < 0.0001$ ) and frequencies of the subtypes (3G, DN,  $p = 0.0062$ ; DP,  $p = 0.0328$ ). This experiment was performed 2 times with at least 3 mice per group. P values are shown.

<https://doi.org/10.1371/journal.pone.0261770.g003>

### The naïve, but not memory T-cell subset, is reduced in secondary lymphoid tissues of $p63^{TECKo}$ mice and contracts over time in postnatal mice

Previous studies were unable to examine the peripheral T-cell compartment due to the rapid mortality of nonconditional p63 deficient mice that die within hours after birth [12]. To assess the peripheral compartment, spleen and lymph node T-cell constituency were quantified in 2-month-old mice. In order to address peripheral homeostasis, we further categorized CD4 and CD8 T-cells into naïve (CD62L+CD44-) and memory (CD62Llo or CD62Lhi, CD44hi) subsets. Despite severe thymic atrophy by the newborn stage in  $p63^{TECKo}$  mice, there was no difference between the groups in total CD8 cell number in either the spleen or lymph nodes (Fig 4A). There was a 10-fold reduction in CD8 naïve T-cells in the spleen (Fig 4B,  $p = 0.0003$ ) with no differences in the CD8 memory compartment (Fig 4C) in  $p63^{TECKo}$  mice. In the CD4 compartment of  $p63^{TECKo}$  mice, there were significantly fewer CD4 T-cells in the spleen ( $p = 0.0031$ ), but not in lymph nodes (Fig 4D). Naïve CD4 T-cells were significantly decreased by 10-fold in both the spleen and lymph node of  $p63^{TECKo}$  mice (Fig 4E). As seen for CD8 T-

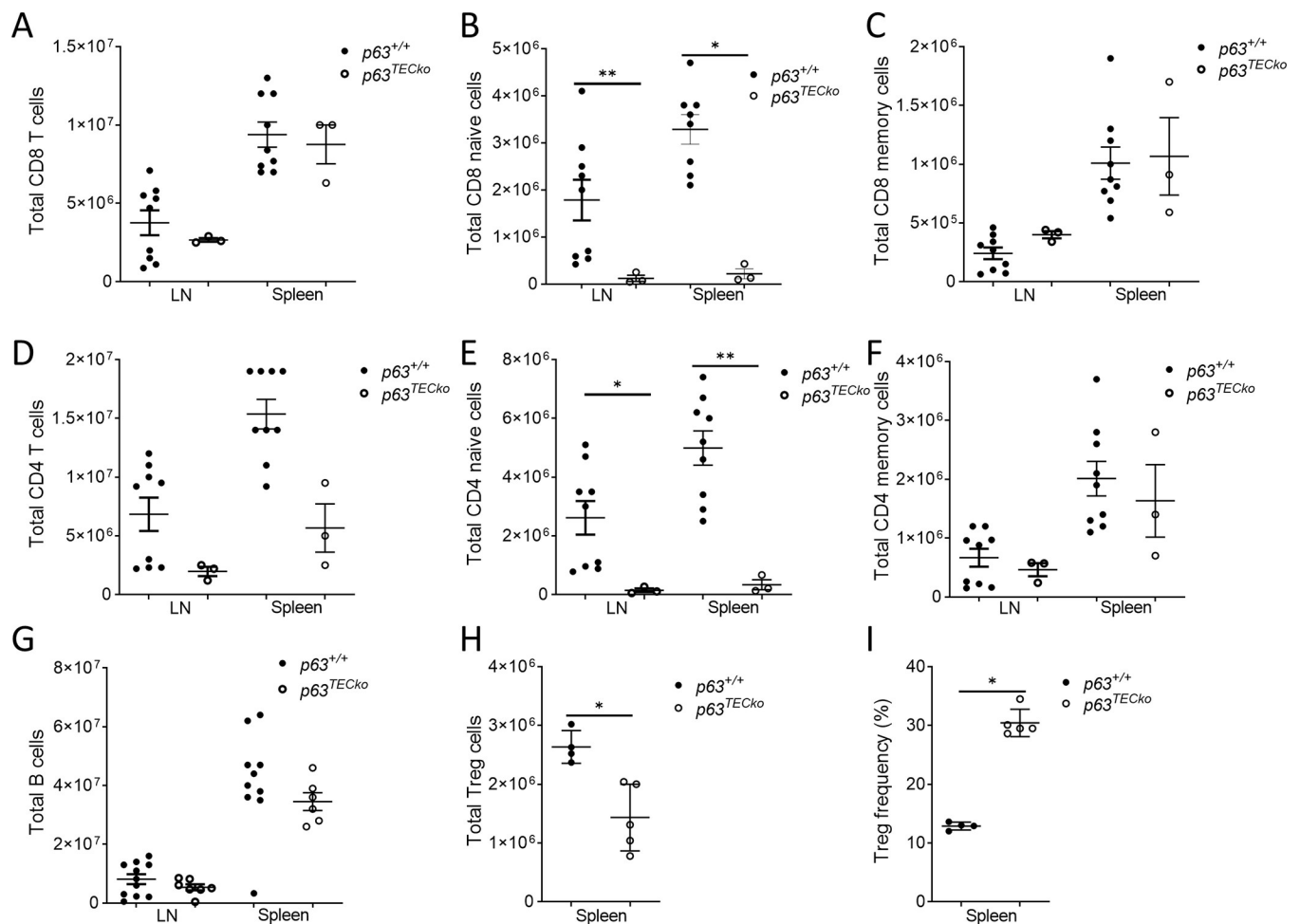


**Fig 4. The peripheral T cell compartment shows decreased naïve cells in  $p63^{TECKo}$  mice.** Flow cytometric analysis for the cell-surface expression of CD4 and CD8 splenocytes and lymphocytes were isolated  $p63^{TECKo}$  and littermate controls. Regulatory T cells were defined as  $CD4^+CD25^{bright}$  and  $FoxP3^+$ . Numbers denote absolute number of cells. (Total CD8 (4A), CD8 naïve (4B; LN,  $p = 0.0573$ ; spleen,  $p = 0.0003$ ), CD8 memory (4C), total CD4(4D; spleen,  $p = 0.0031$ ), CD4 naïve (4E; LN,  $p = .0370$ ; spleen,  $p = 0.0013$ ), CD4 memory (4F), B cells (4G), Treg (4H,  $p = 0.0159$ ) and frequency of Treg (4I,  $p = 0.0159$ ). This experiment was done at least twice with at least three mice per group. P values are shown.

<https://doi.org/10.1371/journal.pone.0261770.g004>

cells in  $p63^{\text{TECKo}}$  mice, there was not a difference in memory CD4 T-cells (Fig 4F) between the groups. Of the other populations examined, TEC p63 deficiency did not alter the absolute numbers of splenic B-cells in the lymph node, while slightly reducing absolute splenic B-cells (Fig 4G). The number of regulatory T cells (Treg; defined as CD4+25bright and FoxP3+) as well as the frequency of Tregs was reduced in  $p63^{\text{TECKo}}$  mice when compared to  $p63^{+/+}$  (Fig 4H and 4I;  $P = 0.0159$ ,  $P = 0.0159$ , respectively). This data shows that p63 expression is required for peripheral maintenance of naïve T cells but not required for the persistence of memory T cells.

### $p63^{\text{TECKo}}$ mice have abnormal patches of skin and absent hair follicles

It is known that p63 is expressed in keratinocytes [10] and p63 knockout mice have a complete loss of stratified epithelium [12]. In addition, the epidermis in p63 knockout mice is non-continuous and fragmented compared to  $p63^{+/+}$  [12]. *FOXN1* deficiency results in a “nude” mouse. These mice are hairless not due to a lack of hair follicles but because these follicles have an absence of free sulfhydryl groups in the mid-follicle region and the hair twists and coils [19]. Although *FOXN1* is not expressed in epithelial stem cells of the skin, *FOXN1* expression is important in terminal differentiation of epithelium [20], leaving the possibility that skin lesions would occur as a result of terminally differentiated stratified epithelium loss. In  $p63^{\text{TECKo}}$  mice, there were no differences in skin at E15.5 or newborn stage compared to  $p63^{+/+}$  (S4 Fig). However, by 2 months of age, surprisingly, 100% of  $p63^{\text{TECKo}}$  mice had abnormal patches of skin that showed no hair (Fig 5A and 5B). We next wanted to assess p63 protein expression between the groups. As shown in Fig 5C and 5D, p63 (shown in red) is abundant in both littermate control and  $p63^{\text{TECKo}}$  skin epidermis. In addition, the skin of  $p63^{\text{TECKo}}$  mice shows continuous epidermis (Fig 5C). Neither  $p63^{\text{TECKo}}$  skin or  $p63^{+/+}$  skin expressed EpCAM (Fig 5E and 5F). There were no differences in other skin antigens between  $p63^{\text{TECKo}}$  mice and their  $p63^{+/+}$  including Cytokeratin 5 (Fig 5C and 5D), Ki67 (Fig 5E and 5F) or loricrin, a terminal differentiation marker in keratinocytes (Fig 5G and 5H) [14]. In assessing the differences based on hematoxylin and eosin staining,  $p63^{\text{TECKo}}$  mice showed that there was an absence of hair follicles which are lined typically with stratified epithelium, compared to  $p63^{+/+}$  (Fig 5I and 5J). Taken together, these data show that the hair follicles in  $p63^{\text{TECKo}}$  mice are the only areas profoundly affected in the skin. This hair loss is due to the absence of hair follicles and not because of a loss of sulfhydryl groups as in Nude mice.

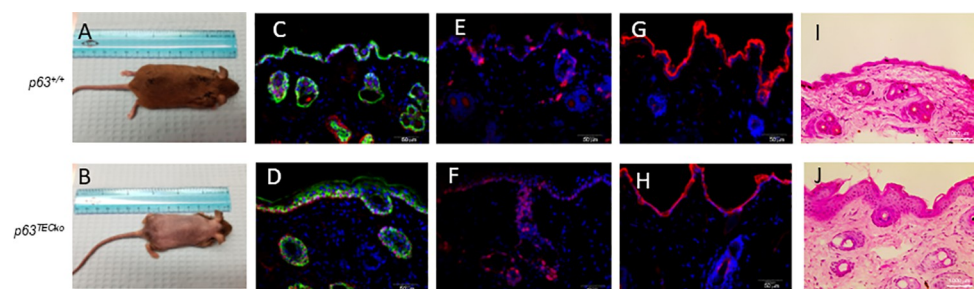


**Fig 5.  $p63^{\text{TECKo}}$  mice have abnormal patches of skin and absent hair follicles.**  $p63^{\text{TECKo}}$  mice are hairless compared to  $p63^{+/+}$  mice (5B and 5A respectively). Fig 5C and 5D shows Cytokeratin 5 (green), p63 (red) and DAPI (blue); Fig 5E and 5F shows Epcam1 (green), Ki67 (red) and DAPI (blue); Fig 5G and 5H shows Loricrin (red) and DAPI (blue); H and E staining of  $p63^{\text{TECKo}}$  mice show the absence of hair follicles (Fig 5I and 5J). The scale bars are 50  $\mu\text{m}$  in 5C to 5H, and 1000  $\mu\text{m}$  in 5I and 5J. This experiment was performed at least twice with at least three mice per group each time.

<https://doi.org/10.1371/journal.pone.0261770.g005>

## Discussion

Our data has shown that loss of p63 expression in TECs causes catastrophic loss of thymocytes. Decreases in TECs did not result in abnormal numbers of thymocytes at E15.5 in p63<sup>TECko</sup> mice. However, in post-natal mice, there was significant thymic hypoplasia in the thymocyte compartment in all subsets. These data indicate that p63 function is critical in TECs to ensure normal thymocyte differentiation. Moreover, normal p63 expression is also required for normal T cell maintenance.

In p63<sup>TECko</sup> mice, 100% of mice by 2 months of age have abnormal patches of skin suggesting that different regulatory elements were responsible for FOXN1 expression and hence p63 expression in these mice. p63 is found in the interfollicular epidermal stem cells and is important for stem cell proliferation [21]. The syndrome called AEC (ankyloblepharon-ectodermal defects-clefting) is an autosomal dominant ectodermal dysplasia disorder caused by mutations in the transcription factor p63 which can clinically manifest in alopecia or sparse hair [22]. We hypothesize that despite p63 being expressed in the stem cells, it was most likely not expressed in the hair follicle stem cells or key progeny, resulting in absence of hair follicles in p63<sup>TECko</sup> mice.

There have been multiple models which explored the role of p63 in development. In the complete p63 knockout mice, major defects in limb, craniofacial and epithelial development, a severely abnormal thymus and absence of all squamous epithelium were noted [12]. Koster et al showed that p63 plays a dual role in development: initiating epithelial stratification and maintaining proliferative potential of basal keratinocytes in mature epidermis [10]. This was reinforced by Truong et al who showed that down-regulation of p63 in keratinocytes using specific siRNAs resulted in severe tissue hypoplasia and inhibited both stratification and differentiation in a cell-autonomous manner in keratinocytes [13]. It is known that disruption of FoxN1 function in mice leads to a profound immune deficiency and a hairless phenotype [23]. FoxN1 deletion in human also results in a catastrophic T cell deficiency, congenital alopecia and nail dystrophy [19]. In a recent study, Larsen and colleagues found a *cis*-regulatory element that was critical for expression of *Foxn1* in TECs but dispensable for expression in hair follicles; in these mice, *Foxn1* expression and function in the hair follicle were unaffected [24].

In p63<sup>TECko</sup> mice, p63 deficiency was restricted to TECs and had severe thymic hypoplasia. These data emphasized the importance of p63 in TECs resulting in the loss of both TECs and thymocytes, most likely as result of the absence of crosstalk that produces bidirectional signaling between TECs and thymocytes, critical in maintaining the thymic microenvironment [24–28]. Senoo et al showed severe thymic hypoplasia in p63 knockout mice; they also observed that K5 and K8 as well as UEA-1 [25–27] expression patterns were indistinguishable between littermate and p63 knockout thymuses at E15.5 [12]. The authors further proved that the thymic defect occurred as a consequence of p63 deficiency in TECs and not in the lymphoid compartment as Rag2-deficient mice that lack mature B and T cells exhibited normal thymic development when reconstituted with p63 knockout hematopoietic stem cells. Thymus hypoplasia was attributed to loss of proliferative potential of thymic epithelial stem cells and enhanced TEC apoptosis. Our data support and further this point by showing the importance of p63 expression in TECs. Taken together our data suggest that p63 is not only important in TEC integrity, but also in preventing thymic involution and in development and maintenance of hair follicles (see S5 Fig).

## Supporting information

**S1 Fig. Representative flow cytometry plots are shown for mTEC and cTEC in E15.5 (S1A Fig) and neonate (S1B Fig) p63+/+ and p63TECko mice.** mTEC are defined as Ly51<sup>+</sup>UEA1<sup>+</sup> and cTEC are defined as Ly51<sup>+</sup>UEA1<sup>-</sup>. Representative flow cytometry plots are shown for

thymic CD4 and CD8 expression profiles in E15.5 (S1C Fig) and neonate (S1D Fig) mice. (TIF)

**S2 Fig. p63<sup>TECko</sup> mice have reduced TEC proliferation.** Absolute numbers (S2A Fig; cTEC,  $p = 0.0026$ ; mTEC,  $p = <0.0001$ ) and frequency (S2B Fig; cTEC,  $p = 0.0001$ ; mTEC,  $p = 0.0011$ ) of TEC subsets were reduced in p63<sup>TECko</sup> compared to p63<sup>+/+</sup> controls. This reduction in both mTECs and cTECs correlated with reduced proliferative potential of TECs in p63<sup>TECko</sup> mice (S2C Fig; cTEC,  $p = 0.0123$ ; mTEC,  $p = 0.0386$ ), but no change in Caspase-3 expression (S2D Fig; mTEC,  $p = 0.0264$ ) within TEC subsets. P values are shown. (TIF)

**S3 Fig. p63<sup>TECko</sup> mice have a profound reduction in Treg absolute numbers and frequencies.** Total number (3A;  $p < 0.0001$ ) and frequency of FoxP3<sup>+</sup> Treg (3B;  $p = 0.0184$ ). P values are shown. (TIF)

**S4 Fig. E15.5 and newborn p63<sup>TECko</sup> mice didn't show any visible hair loss in skin compared to their p63<sup>+/+</sup> littermates.** Panels A-D shows Cytokeratin 5 (green), p63 (red) and DAPI (blue); Panels E-H show Ki67 (red) and DAPI (blue); Panels I-L shows Loricrin (red) and DAPI (blue); Panels M-P show H and E staining of skin at E15.5 and Newborn timepoints. (TIF)

**S5 Fig. Graphical summary of the key differences and similarities in thymic phenotype upon TEC-specific p63 deletion in E15.5 and neonate mice.** (TIF)

**S1 Data.**  
(XLSX)

## Author Contributions

**Conceptualization:** Heather E. Stefanski, Emily Goren, Georg A. Hollander, Bruce R. Blazar.

**Data curation:** Heather E. Stefanski, Jemma Nicholls.

**Formal analysis:** Heather E. Stefanski, John McGrath.

**Funding acquisition:** Georg A. Hollander, Bruce R. Blazar.

**Investigation:** Heather E. Stefanski, Yan Xing, Leslie Jonart, Emily Goren, Patricia A. Taylor, Megan Riddle, Jakub Tolar.

**Methodology:** John McGrath.

**Resources:** Alea A. Mills, Georg A. Hollander, Bruce R. Blazar.

**Writing – original draft:** Heather E. Stefanski.

**Writing – review & editing:** Heather E. Stefanski, Yan Xing, Jemma Nicholls, Leslie Jonart, Emily Goren, Patricia A. Taylor, Alea A. Mills, Megan Riddle, John McGrath, Jakub Tolar, Georg A. Hollander, Bruce R. Blazar.

## References

1. van Ewijk W., Wang B., Hollander G., Kawamoto H., Spanopoulou E., Itoi M., et al. 1999. Thymic micro-environments, 3-D versus 2-D? *Semin Immunol* 11: 57–64. <https://doi.org/10.1006/smim.1998.0158> PMID: 9950752

2. Starr T. K., Jameson S. C., and Hogquist K. A. 2003. Positive and negative selection of T cells. *Annu Rev Immunol* 21: 139–176. <https://doi.org/10.1146/annurev.immunol.21.120601.141107> PMID: 12414722
3. Petrie H. T., and Zuniga-Pflucker J. C. 2007. Zoned out: functional mapping of stromal signaling micro-environments in the thymus. *Annu Rev Immunol* 25: 649–679. <https://doi.org/10.1146/annurev.immunol.23.021704.115715> PMID: 17291187
4. Sawicka M., Stritesky G. L., Reynolds J., Abourashchi N., Lythe G., Molina-París C., et al. 2014. From pre-DP, post-DP, SP4, and SP8 Thymocyte Cell Counts to a Dynamical Model of Cortical and Medullary Selection. *Frontiers in immunology* 5: 19–19. <https://doi.org/10.3389/fimmu.2014.00019> PMID: 24592261
5. Siggs O. M., Makaroff L. E., and Liston A. 2006. The why and how of thymocyte negative selection. *Curr Opin Immunol* 18: 175–183. <https://doi.org/10.1016/j.coi.2006.01.001> PMID: 16459069
6. Chilosi M., Zamo A., Brighenti A., Malpeli G., Montagna L., Piccoli P., et al. 2003. Constitutive expression of DeltaN-p63alpha isoform in human thymus and thymic epithelial tumours. *Virchows Archiv. an international journal of pathology* 443: 175–183. <https://doi.org/10.1007/s00428-003-0857-4> PMID: 12851817
7. Guo X., and Mills A. A. 2007. p63, Cellular Senescence and Tumor Development. *Cell Cycle* 6: 305–311. <https://doi.org/10.4161/cc.6.3.3794> PMID: 17224650
8. Keyes W. M., Wu Y., Vogel H., Guo X., Lowe S. W., and Mills A. A. 2005. p63 deficiency activates a program of cellular senescence and leads to accelerated aging. *Genes Dev* 19: 1986–1999. <https://doi.org/10.1101/gad.342305> PMID: 16107615
9. Yang A., Kaghad M., Wang Y., Gillett E., Fleming M. D., Dotsch V., et al. 1998. p63, a p53 homolog at 3q27–29, encodes multiple products with transactivating, death-inducing, and dominant-negative activities. *Mol Cell* 2: 305–316. [https://doi.org/10.1016/s1097-2765\(00\)80275-0](https://doi.org/10.1016/s1097-2765(00)80275-0) PMID: 9774969
10. Koster M. I., Kim S., Mills A. A., DeMayo F. J., and Roop D. R. 2004. p63 is the molecular switch for initiation of an epithelial stratification program. *Genes Dev* 18: 126–131. <https://doi.org/10.1101/gad.1165104> PMID: 14729569
11. Di Como C. J., Urist M. J., Babayan I., Drobnyak M., Hedvat C. V., Teruya-Feldstein J., et al. 2002. p63 expression profiles in human normal and tumor tissues. *Clinical cancer research: an official journal of the American Association for Cancer Research* 8: 494–501.
12. Senoo M., Pinto F., Crum C. P., and McKeon F. 2007. p63 Is essential for the proliferative potential of stem cells in stratified epithelia. *Cell* 129: 523–536. <https://doi.org/10.1016/j.cell.2007.02.045> PMID: 17482546
13. Truong A. B., Kretz M., Ridky T. W., Kimmel R., and Khavari P. A. 2006. p63 regulates proliferation and differentiation of developmentally mature keratinocytes. *Genes Dev* 20: 3185–3197. <https://doi.org/10.1101/gad.1463206> PMID: 17114587
14. Mills A. A., Zheng B., Wang X.-J., Vogel H., Roop D. R., and Bradley A. 1999. p63 is a p53 homologue required for limb and epidermal morphogenesis. *Nature* 398: 708. <https://doi.org/10.1038/19531> PMID: 10227293
15. Mills A. A., Qi Y., and Bradley A. 2002. Conditional inactivation of p63 by Cre-mediated excision. *Genesis* 32: 138–141. <https://doi.org/10.1002/gene.10067> PMID: 11857801
16. Zuklys S., Gill J., Keller M. P., Hauri-Hohl M., Zhanybekova S., Balciunaite G., et al. 2009. Stabilized beta-catenin in thymic epithelial cells blocks thymus development and function. *J Immunol* 182: 2997–3007. <https://doi.org/10.4049/jimmunol.0713723> PMID: 19234195
17. Xing Y., and Hogquist K. A. 2014. Isolation, identification, and purification of murine thymic epithelial cells. *Journal of visualized experiments: JoVE*: e51780. <https://doi.org/10.3791/51780> PMID: 25145384
18. Anderson G., and Jenkinson E. J. 2001. Lymphostromal interactions in thymic development and function. *Nat Rev Immunol* 1: 31–40. <https://doi.org/10.1038/35095500> PMID: 11905812
19. Gallo V., Cirillo E., Giardino G., and Pignata C. 2017. FOXP1 Deficiency: from the Discovery to Novel Therapeutic Approaches. *J Clin Immunol* 37: 751–758. <https://doi.org/10.1007/s10875-017-0445-z> PMID: 28932937
20. Baxter R. M., and Brissette J. L. 2002. Role of the Nude Gene in Epithelial Terminal Differentiation. *Journal of Investigative Dermatology* 118: 303–309. <https://doi.org/10.1046/j.0022-202x.2001.01662.x> PMID: 11841548
21. Fuchs E., and Horsley V. 2008. More than one way to skin. *Genes & development* 22: 976–985.
22. Clements S. E., Techanukul T., Lai-Cheong J. E., Mee J. B., South A. P., Pourreynon C., et al. 2012. Mutations in AEC syndrome skin reveal a role for p63 in basement membrane adhesion, skin barrier integrity and hair follicle biology. *Br J Dermatol* 167: 134–144. <https://doi.org/10.1111/j.1365-2133.2012.10888.x> PMID: 22329826

23. Cheng L., Guo J., Sun L., Fu J., Barnes P. F., Metzger D., et al. 2010. Postnatal tissue-specific disruption of transcription factor FoxN1 triggers acute thymic atrophy. *J Biol Chem* 285: 5836–5847. <https://doi.org/10.1074/jbc.M109.072124> PMID: 19955175
24. Larsen B. M., Cowan J. E., Wang Y., Tanaka Y., Zhao Y., Voisin B., et al. 2019. Identification of an Intronic Regulatory Element Necessary for Tissue-Specific Expression of Foxn1 in Thymic Epithelial Cells. *J Immunol* 203: 686–695. <https://doi.org/10.4049/jimmunol.1801540> PMID: 31243087
25. Shores E. W., Van Ewijk W., and Singer A. 1991. Disorganization and restoration of thymic medullary epithelial cells in T cell receptor-negative scid mice: Evidence that receptor-bearing lymphocytes influence maturation of the thymic microenvironment. *European Journal of Immunology* 21: 1657–1661. <https://doi.org/10.1002/eji.1830210711> PMID: 2060577
26. Shores E. W., Van Ewijk W., and Singer A. 1994. Maturation of medullary thymic epithelium requires thymocytes expressing fully assembled CD3-TCR complexes. *International Immunology* 6: 1393–1402. <https://doi.org/10.1093/intimm/6.9.1393> PMID: 7819148
27. van Ewijk W., Shores E. W., and Singer A. 1994. Crosstalk in the mouse thymus. *Immunology Today* 15: 214–217. [https://doi.org/10.1016/0167-5699\(94\)90246-1](https://doi.org/10.1016/0167-5699(94)90246-1) PMID: 8024681
28. Lopes N., Serge A., Ferrier P., and Irla M. 2015. Thymic Crosstalk Coordinates Medulla Organization and T-Cell Tolerance Induction. *Front Immunol* 6: 365. <https://doi.org/10.3389/fimmu.2015.00365> PMID: 26257733